photonics

MDPI

Communication

Improvement of Efficiency in 976 nm Fiber Amplifier by Spectral Filtering in Yb-Doped Fiber with Absorbing Rods Embedded in the Cladding

Svetlana S. Aleshkina [1], Danila A. Davydov [1], Vladimir V. Velmiskin [1], Mikhail V. Yashkov [2], Andrey A. Umnikov [2], Sergey V. Alyshev [1], Liudmila D. Iskhakova [1], Mikhail M. Bubnov [1], Denis S. Lipatov [2] and Mikhail E. Likhachev [1,*]

[1] Prokhorov General Physics Institute of the Russian Academy of Sciences, Dianov Fiber Optics Research Center, 119333 Moscow, Russia; sv_alesh@fo.gpi.ru (S.S.A.); gaufleiche@fo.gpi.ru (D.A.D.); vvv@fo.gpi.ru (V.V.V.); alyshs@fo.gpi.ru (S.V.A.); ldisk@fo.gpi.ru (L.D.I.); bubnov@fo.gpi.ru (M.M.B.)
[2] Devyatykh Institute of Chemistry of High-Purity Substances of the Russian Academy of Sciences, 49 Tropinina St., 603951 Nizhny Novgorod, Russia; yashkov@ihps-nnov.ru (M.V.Y.); umnikov@ihps-nnov.ru (A.A.U.); lipatov@ihps-nnov.ru (D.S.L.)
* Correspondence: likhachev@fo.gpi.ru

Abstract: A novel Yb-doped fiber design for improved lasing near 976 nm based on spectral filtering of the amplified spontaneous emission near 1030 nm was realized and investigated. A very sharp short-pass filter was implemented by adding appropriately chosen high-index absorbing rods into the silica cladding. In this case, the resonant interaction of the core mode with the high-index rod mode could be controlled by fiber bending, which allows for the precise adjustment of the stop-band position. It was shown that the utilization of Sm-doped absorbing rods allows one to achieve very high absorption of emission at unwanted wavelengths, but it also adds background losses for the pump near 915 nm and for the signal at 976 nm. Despite this fact, the improvement of efficiency in the 976 nm fiber amplifier, after shifting the stop-band to 1000 nm, was clearly demonstrated. Based on theoretical calculations, it was shown that, after optimizing the fiber parameters, a further twofold improvement in efficiency was possible despite the excess losses at the pump and signal wavelengths.

Keywords: spectral filtering; Yb-doped fiber amplifier; fiber optimization; 976 nm fiber laser

Citation: Aleshkina, S.S.; Davydov, D.A.; Velmiskin, V.V.; Yashkov, M.V.; Umnikov, A.A.; Alyshev, S.V.; Iskhakova, L.D.; Bubnov, M.M.; Lipatov, D.S.; Likhachev, M.E. Improvement of Efficiency in 976 nm Fiber Amplifier by Spectral Filtering in Yb-Doped Fiber with Absorbing Rods Embedded in the Cladding. *Photonics* **2024**, *11*, 89. https://doi.org/10.3390/photonics11010089

Received: 28 November 2023
Revised: 30 December 2023
Accepted: 15 January 2024
Published: 17 January 2024

1. Introduction

The extensively growing number of applications of fiber lasers requires an expansion of the operating wavelength range. For example, Yb-doped fiber lasers that operate near 976 nm are of great interest as potential high-power single-mode pump sources for Er- and Yb-doped lasers. They are also very promising for frequency doubling (to replace inefficient and expensive Ar lasers) and frequency quadrupling (to replace excimer lasers for fiber Bragg grating whitening). At the same time, it is very difficult to achieve efficient lasing in Yb-doped fibers outside the wavelength range of 1020–1090 nm. The reason for this is that, for short-wavelength operation (near 976 nm), it is necessary to suppress the amplified spontaneous emission (ASE) near 1030 nm, which typically has the lowest lasing threshold in standard fibers. There are plenty of works regarding this topic to date [1–8]. The most promising results so far have been demonstrated by fabricating a short-pass filter based on the rather complicated Photonics Bandgap Fiber design [4,5]. In this case, the fiber parameters are chosen in such a way that the emission at 976 nm belongs to the bandgap region, and thus, the core mode at 976 nm is exactly confined to the core region. Emission at wavelengths longer than 1 μm is in the region of the permitted zone and cannot be localized in the core (the overlap integral of the longitudinal modes with a doped region is significantly reduced).

Previously, we proposed a much simpler fiber design based on adding absorbing rods into the cladding and adjusting fiber parameters to achieve resonant coupling of the core mode with absorbing-rod modes at the unwanted wavelength [9]. Theoretical and experimental analyses have demonstrated the possibility of precisely controlling the position of the stop-band in such fibers by its bending. Moreover, a very sharp transition from the low-loss to the high-loss spectral region was previously demonstrated (optical losses were changed by two orders of magnitude for a wavelength region of only 12 nm) [9].

The aim of the current work was to investigate the possibility of applying the proposed technique for improving the pump-to-signal conversion efficiency (PCE) in Yb-doped fiber lasers that operate near 976 nm. It was demonstrated for the first time that the limiting factor in this case is the increase of cladding loss at the pump wavelength due to absorption in the rods and the increase of signal loss at 976 nm due to the stop-band edge. Careful optimization of the fiber design demonstrated the possibility of overcoming this limitation by choosing an appropriate concentration of Yb ions in the fiber core. It was shown, theoretically, that the implementation of this approach improved the efficiency by a factor of two compared to the fiber without absorbing rods.

2. Materials and Methods

The aim of the current work was to fabricate a Yb-doped fiber with suppressed fundamental mode propagation at wavelengths above 1000 nm and to test such a fiber in the configuration of an amplifier operating near 976 nm. To achieve a sharp long-wavelength stop-band, we used a fiber design with three absorbing rods embedded into the cladding, proposed earlier in [9]. The designed core parameters were chosen as follows: core-cladding index difference (dn) ~0.0017, core diameter = 11 μm, cladding diameter ~80 μm. The core parameters were chosen to achieve the maximum core diameter near the single-mode operation regime, but to keep the bending sensitivity reasonably low. The cladding diameter of the active fiber was reduced down to 80 μm to increase the pump absorption (and therefore, PCE). This became possible because, for the experiment, we used a pump and signal combiner in configuration 2 + 1 to 1 based on passive fiber with a cladding diameter of 80 μm. In this case, the pump of two 105/125 μm fibers with numerical aperture 0.22 was side-coupled with 85% efficiency to a 10/80 μm passive fiber coated with low-index polymer provided NA > 0.45. The absorbing rods were chosen to have a diameter of 3.1 μm, dn = 0.010, and distance from the fiber axis of 20 μm to achieve the stop-band in the bend fiber at a wavelength of 1000 nm and longer (similar to that in [9]).

2.1. Fabricattion of Yb-Doped Fiber with Absorbing Rods Emdedded into the Cladding

The fiber preform was fabricated in three steps: the fabrication of the Yb-doped core rod, the fabrication of Sm-doped absorbing rods, and the consolidation of Yb-doped preform with Sm-doped rods. The Yb-doped preform was fabricated using the combined all-gas-phase Modified Chemical Vapor Deposition (MCVD) technique as described below. High-purity Heraeus Suprasil F300 tubes were taken as substrate tubes. As precursors, high-purity, high-volatile $SiCl_4$, $POCl_3$, $C_2F_3Cl_3$, CCl_4, and low-volatile solid powders of $AlCl_3$, $Yb(tmhd)_3$ (with 5 N purity) were used. In order to achieve all-gas-phase deposition, we used containers with $AlCl_3$ and $Yb(thmd)_3$ powders, which were heated up to the temperature of 130 и 160 °C correspondingly. In this case, vaporized precursors were delivered to the reaction zone through separate heated lines by carrier gas argon.

First $F/Yb_2O_3/Al_2O_3/SiO_2$-core preform was fabricated by this method. The concentration of Al_2O_3 was chosen to be ~2 mol.%. To reduce the core-cladding refractive index difference (dn) to the level of 0.0017, we added ~0.3 wt.% of F to the core glass. The concentration of Yb was low enough (~0.06 wt.%) to not significantly affect the core refractive index. This concentration of Yb was chosen to provide a relatively long optimal length of the fiber in amplifier configuration (according to our calculations ~10 m), which guaranteed that the loss of the fundamental mode due to resonant coupling at wavelengths above 1000 nm would be sufficient to completely suppress ASE near 1030 nm. In addition, the relatively low concentration of Yb ensured immunity to the photodarkening effect. The Yb-doped rod was jacketed by an F300 Heraeus tube to obtain the required core/cladding ratio.

An Sm-doped absorption rod was fabricated by a combined gas-phase and solution-doping MCVD technique, which consisted of the following steps. A porous glass layer of SiO_2-Al_2O_3 was deposited on the inner surface of the high-purity silica glass tube (Heraeus F300, Hanau, Germany). Both reagents were deposited from the gas phase. Doping of the porous layer was performed with an aqueous-alcohol solution of $Sm(NO_3)_3$ followed by drying of the porous glass. In the final stage, the porous layer was sintered into transparent glass, and the tube with the deposited Sm-doped core layer was consolidated into a glass rod. The core-cladding refractive index difference in the fabricated preform was 0.010. An analysis, performed with the help of energy-dispersive X-ray spectroscopy (AZtecENERGY analytical systems; Oxford Instruments, Abingdon, UK; JSM5910-LV, JEOL, Tokyo, Japan), showed that the core was doped with ~4 wt.% of Sm and 1.4 mol.% of Al_2O_3 (sufficient to suppress the gray loss level coursed by Sm^{3+} ions clustering). Doping with Sm was chosen due to its intense absorption band at 1080 nm, which also covers the region up to 1000 nm. The minimum optical loss of Sm ions was at 982 nm, which is very close to our signal wavelength (976 nm). Thus, the utilization of Sm ions as an absorber provided additional (to mode coupling) filtering of ASE at 1030 nm.

In the final step, three holes were drilled around the Yb-doped core, and then, Sm-doped rods, stretched to a diameter to fit these holes, were inserted in. The core/cladding ratio in the Sm-doped rod was adjusted by jacketing with F300 tubes to achieve the designed diameter in the final preform. The preform was consolidated then to a solid glass rod. The fabricated preform had a circular shape, which was not optimal for cladding pumping. For this reason, we polished the preform at the final stage to achieve a square shape of the outer silica cladding.

Fibers with different core and square cladding sizes ($11/80 \times 80$ μm, $13/92 \times 92$ μm, and $15/105 \times 105$ μm) were drawn from the preform. This was performed to test different positions of the stop-band center. For example, in [9], the stop-band center was centered near 1200 nm and then was widened by bending so that the short-wavelength edge of the stop-band reached 1000 nm. In our case, drawing the fibers with different diameters allowed us to choose the optical bending configuration with the lowest bending loss, when the stop-band cover spectral region 1000–1100 nm. The double-clad fibers were coated with a low-index acrylate polymer during the drawing, providing a first cladding NA > 0.45.

2.2. Amplifier Operated near 976 nm

The fabricated fiber was tested in the amplifier setup (see Figure 1). The scheme was based on a simple master-oscillator and power-amplifier configuration, with a co-propagating cladding pump at 915 nm and a signal at 976.5 nm. In such a scheme, the seed from the single-mode semiconductor laser diode, with a central wavelength of 976.5 nm and power up to 60 mW, passed through the isolator and then was coupled to the pump combiner (PC) with an output fiber diameter of about 80 μm. Between the pump combiner and isolator, we added WDM, which separates backward-propagated signals at 1030 nm. This was performed to protect the seed from unwanted ASE generated in the Yb-doped fiber under test (YDF), and it also made it possible to measure the power of the backward-propagated ASE near 1030 nm. The YDF was spliced to the output of the pump combiner. The output end of the YDF was angle-cleaved to prevent back reflection. Measurements of the power at the output of the Yb-fiber were conducted in two steps. First, the cladding pump stripper (CPS) was formed at the end of the fiber. This allowed us to nearly completely remove the unabsorbed pump power and retain only the signal propagating in the fiber core. Then, we separated the amplified signal at 976.5 nm from ASE at 1030 nm using a dichroic mirror (a 976.5 nm signal was reflected by the mirror, and ASE at wavelengths above 1000 nm was passed through). In the second stage, the dichroic mirror and CPS were removed to measure the net power at the output of the YDF. By subtracting the amplified signal and ASE from the net power, we calculated the unabsorbed pump power.

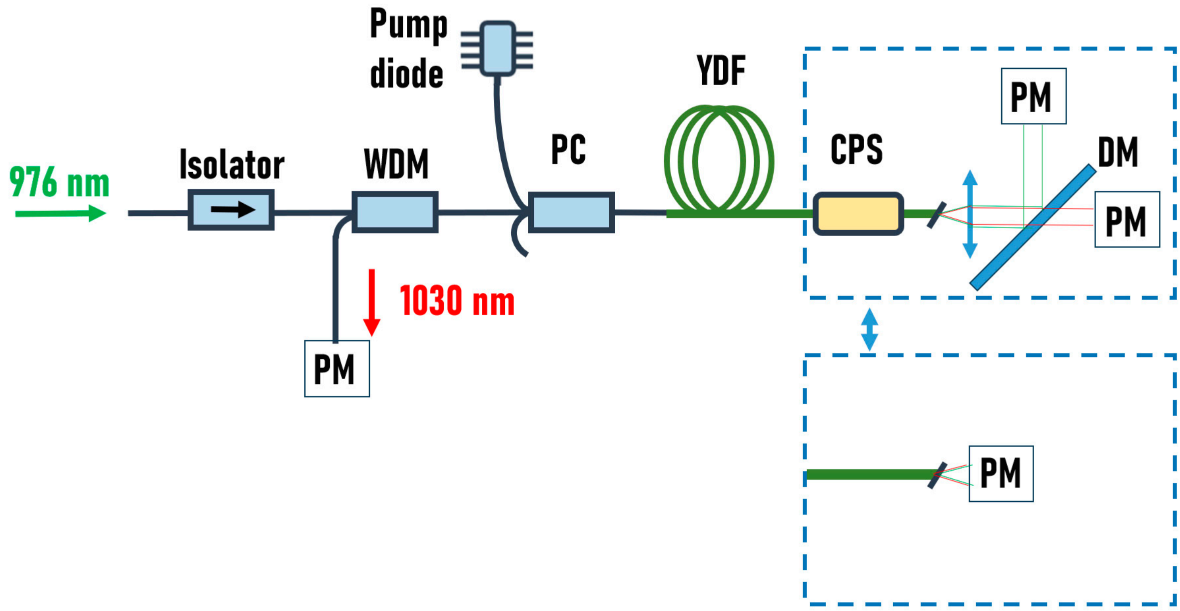

Figure 1. The scheme of the amplifier set-up.

It is worth noting that the amplifier configuration was chosen in our study instead of the laser configuration to avoid uncertainty due to splice loss with the output fiber Bragg grating in the laser configuration. In the case of the amplifier, it was possible to analyze the fiber properties by itself.

3. Results

The refractive index profile, measured in the fabricated fiber with sizes 15/105 × 105 µm, is shown in Figure 2. In the insert to Figure 2, the cross-sectional image of the fabricated fiber is presented. It can be noted that the refractive index of the core became somewhat higher than that of preform (0.0021 instead of 0.0017), which was caused by non-zero drawing tension [10], which was required to keep the shape of the fiber close to square. It should be noted that this increase in dn was not critical since the fiber was designed to be bent during operation (required to widen the stop band [9]), and high-order modes were efficiently evacuated in this case. The refractive index of Sm-doped rods was also changed after drawing—the refractive index difference was reduced down to 0.0095, which we attributed to Al diffusion.

First, the optical losses in the drawn fibers were measured using the standard cut-back technique. For fiber with cladding sizes 15/105 × 105 µm, the center of the stop-band was found at wavelength 1250 nm. In this case, the fiber required tight bending to a diameter less than 60 mm to shift the stop-band down to 1030 nm. The 11/80 × 80 µm fiber had the stop-band at too short of a wavelength (950 nm). Finally, the 13/92 × 92 µm had the center of the stop-band near 1100 nm. Our experiments showed that, with this fiber, it was possible to achieve the sharpest edge of the stop band (see Figure 3). It was possible to precisely control the position of the left edge of the stop-band by bending. In particular, it was possible to achieve medium loss at 1030 nm (~2 dB/m) with very low loss at the signal wavelength (976.5 nm) by bending the fiber with a diameter of 115 mm. Additionally, with a bending diameter of 85 mm, it was possible to almost completely suppress all signals above 1000 nm (optical loss at 1030 nm exceeded 10 dB/m) but at the cost of a slightly increased loss at the signal wavelength (~0.2 dB/m).

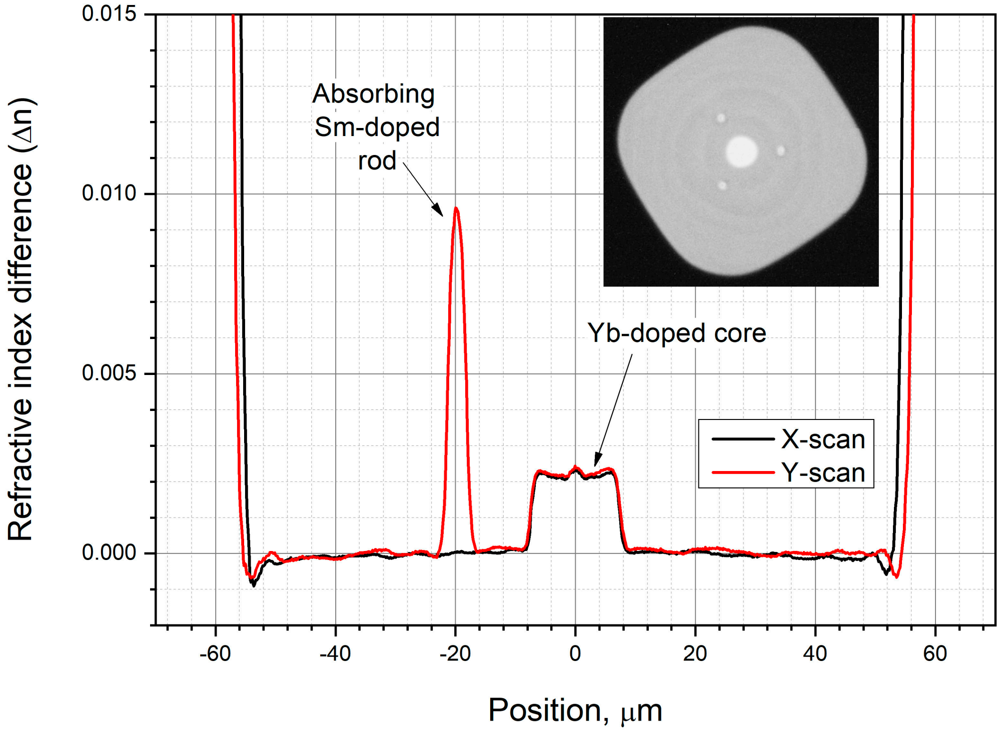

Figure 2. The refractive index profile measured in 15/105 × 105 μm by the fiber analyzer EXFO NR9200HR. The X-scan did not cross the absorption rod; the Y-scan passed through the absorption rod center; insert: fiber cross section, obtained with an optical microscope.

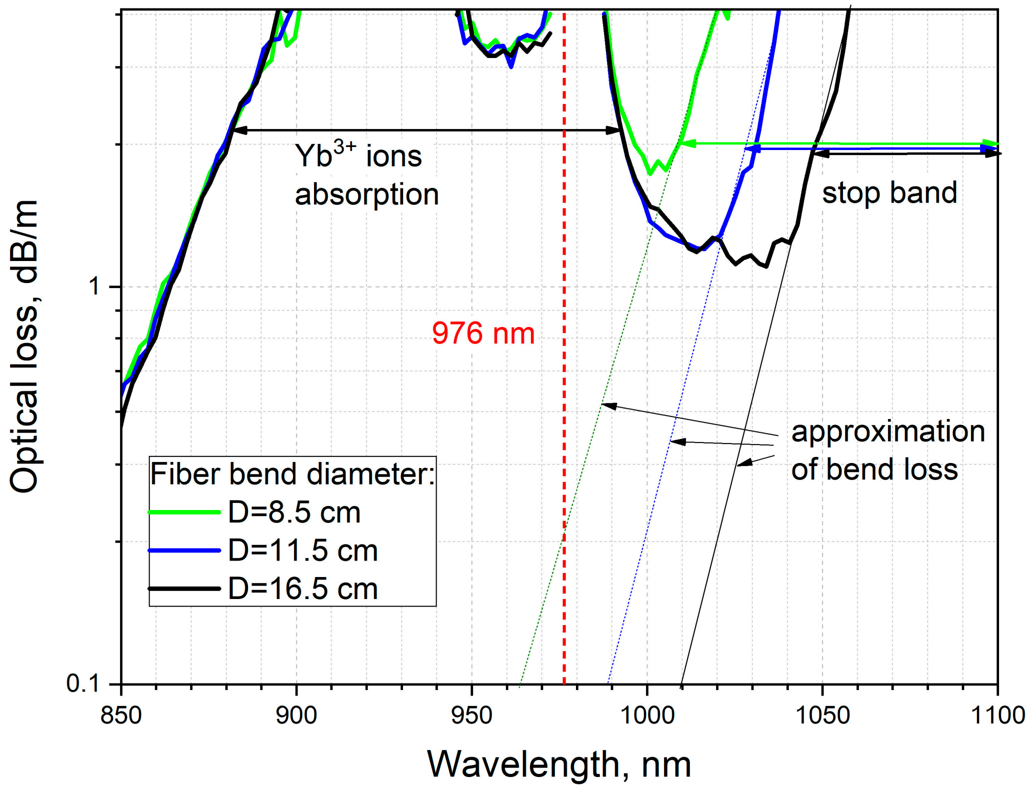

Figure 3. Core loss measured in the 13/92 × 92 μm fiber wound on spools with different diameters.

The cladding absorption measured in the fabricated fiber is shown by the solid black line in Figure 4. Multiple absorption bands could be seen in the spectra. There was a well-known absorption band of Yb^{3+} ions in the spectral region from 850 to 1000 nm. Other bands were associated with the absorption of Sm^{3+} ions in the absorbing rods. To make it clear, we added to Figure 4 the rescaled absorption spectrum measured in the fiber, drawn from the Sm-doped preform (shown by a red dashed line). It can be seen that all the observed absorption peaks corresponded to the peaks of the Sm-doped fiber. Some discrepancy at wavelengths above 1200 nm was due to absorption in the coating polymer at these wavelengths. Sm^{3+} ions also had a low-intensity broad absorption band near 940 nm. This absorption band overlapped with the spectral region of possible pump wavelength. It had quite low intensities (~0.17 dB/m at 940 nm and 0.11 dB/m at 915 nm), but it became comparable with the pump absorption due to a low concentration of Yb in the fabricated fiber. As a result, the PCE of the fiber was reduced due to the loss of pump photons.

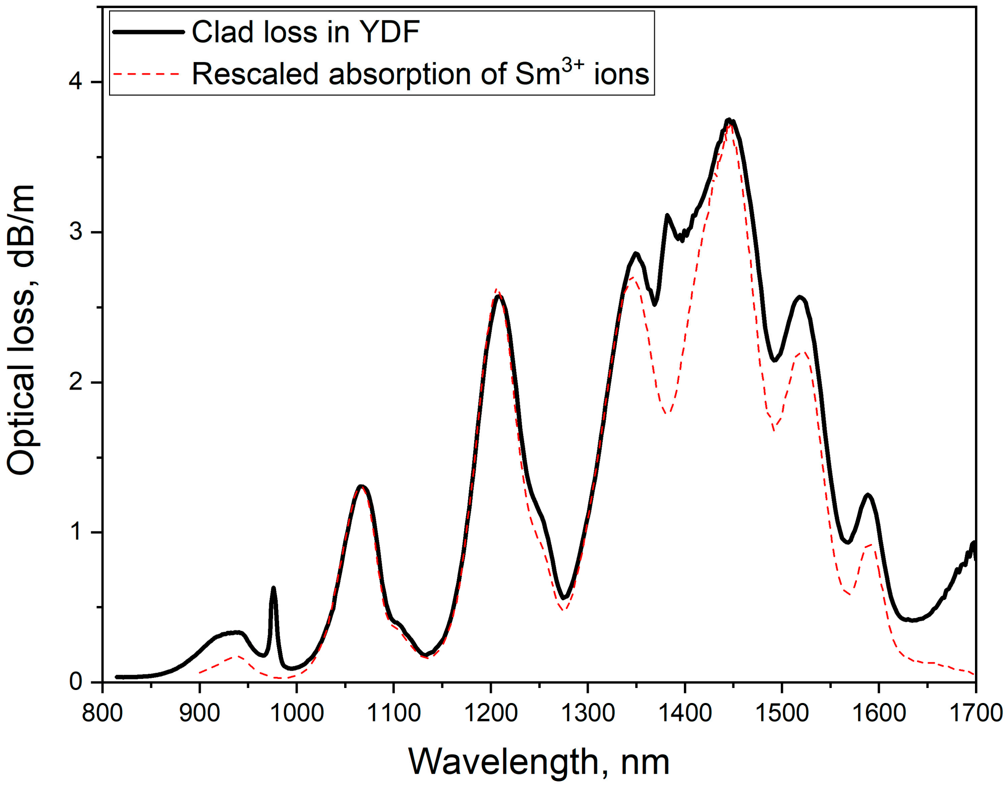

Figure 4. Cladding absorption measured in the fabricated fiber.

The 13/92 × 92 μm fiber was chosen for experiments in the amplifier setup shown in Figure 1. First, we measured the dependence of the amplifier signal power, backward and forward ASE, near 1030 nm on the fiber length when it was wound on a spool with a diameter of ~16 cm. In this case, the stop-band was quite far from the 1030 nm region, and the fiber behavior was close to that which we expected to achieve in the straight fiber or fiber without absorption rods. We used a fixed pump power of 14.6 W @ 915 nm and an input signal power of 60 mW @ 976.5 nm. The obtained results are presented in Figure 5a by solid symbols. The optimal length of the fiber was about 12.5 m, and at longer fiber lengths, strong ASE near 1030 nm, which propagated in both forward and backward directions, had appeared. Slope pump to signal conversion efficiency in this case was estimated to be ~10%.

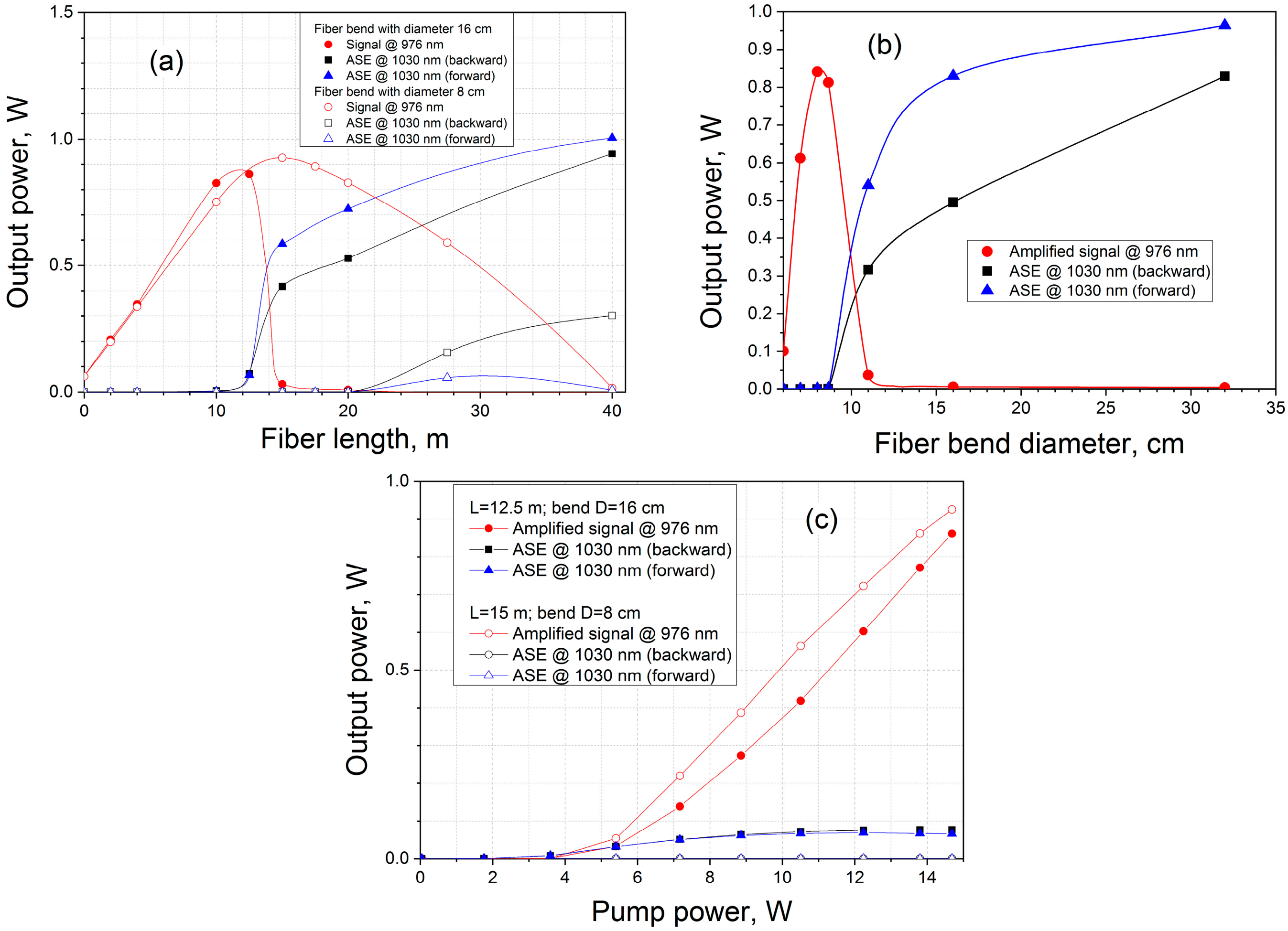

Figure 5. (**a**) Dependence of output power on the 13/92 × 92 µm fiber length; (**b**) dependence of the amplified signal power at the output of 20 m long 13/92 × 92 µm fiber on the fiber's bend diameter; (**c**) dependence of output power (amplified signal at 976 nm and ASE at 1030 nm) on pump power.

Next, we investigated the effect of fiber bending and coursed shift of stop-band to the short wavelength on fiber amplifier efficiency. To find the optimal bend diameter, we selected a fiber length of 20 m, which was long enough for ASE at 1030 nm to be built up in the fiber wound with a large diameter. We then took a set of spools with different diameters and tested the amplifier with the fiber wound on each of these spools. The resulting dependencies of the amplified signal power, backward and forward ASE at 1030 nm, on bend diameter are shown in Figure 5b. It can be clearly seen that, as the diameter of the spool decreased, the power in the ASE near 1030 nm decreased. For diameters below 11 cm, the signal power at 976 nm started to increase and reached its maxima for spool with a diameter of 8 cm. The ASE near 1030 nm was almost completely suppressed by bending in this case. Further reduction of the bend diameter resulted in a decrease of the amplified signal power, which was caused by the shift of the stop-band to the 976 nm wavelength region.

Finally, we selected a spool with diameter of 8 cm as optimal for the suppression of the ASE at 1030 nm and measured the dependence of the output power of the amplified signal and the ASE at 1030 nm on the fiber length. The results of the measurements are shown as open circles in Figure 5a. It can be seen that the optimum fiber length was found to be 15 m, where the maximum amplified signal was obtained. In Figure 5c, it is clearly seen that the use of 15 m long fiber bent with a diameter of 8 cm allowed for an increase in the output power in the whole range of the tested pump power.

4. Discussion

As could be seen in the Section 3 described above, the design of the developed Yb-doped fiber with absorption rods embedded into the cladding allowed for efficient suppression of ASE near 1030 nm by appropriate fiber bending. A clear increase in output signal power was observed in the fabricated fiber. At the same time, the increase of the output signal was rather small, about 10–30% depending on the pump power (see Figure 5). Additionally, the overall efficiency near 10% was still small, and it was comparable to the results obtained in fiber with a ring-doping design, in which no suppression of ASE at 1030 nm was realized [6]. In fact, the main objective of the current work was to test a novel approach to increase PCE in fiber amplifiers that operate near 976 nm and to reveal factors, which limits the applicability of the current method. This step is of great importance before the fiber can be optimized to achieve the maximum efficiency. From our study, we can see that it is possible to indicate two main factors that limit the efficiency of 976 nm amplifiers.

The first factor is the relatively high loss of signal at 976 nm in the bent fiber. As can be seen from Figures 3 and 5, wounding the $13/92 \times 92$ µm fiber on a spool with a diameter of 8–8.5 cm efficiently suppressed the ASE at 1030 nm and increased the signal at 976 nm. At the same time, it added optical loss at 976 nm on the level of 0.2 dB/m (estimated for a bend diameter of 8.5 cm), which was noticeably high, as the length of the fiber used in the amplifier was on the level of 10–20 m. Effects of bending could be clearly seen for the amplifier based on 10 m long fiber (see Figure 5a). In this experiment, the fiber was wound on spools with diameters of 8 and 16 cm. In both cases, the length of the fiber was short enough, and no ASE at 1030 nm appeared. This means that a difference in output power for different bend diameters was secured by additional optical loss, which appeared for fiber wound on the spool with a diameter of 8 cm. The difference was only 10% for a 10 m long fiber, but the decrease in efficiency would be higher for a longer fiber length. We suggest that excess loss at 976 nm was exactly the factor that is responsible for the decrease in signal in fiber wound on the spool with a diameter of 8 cm when its length was increased from 15 to 20 m. Indeed, ASE near 1030 nm at these lengths of fiber is negligibly small and could not affect the amplifier efficiency. The reason for the appearance of these losses is the stop-band edge, which was not sharp enough. It was not possible to reduce excess loss at 976 nm in the current fiber design by increase of fiber bend diameter. In this case, we would have an insufficient shift of the stop-band—not all wavelengths in the region 1000–1030 nm would have a high enough loss, which would result in the decrease of PCE (see Figure 5b). However, the effect of the excess loss could be significantly reduced if the optimal length of the active fiber becomes shorter (by increasing the Yb content in the core).

The second factor is a high cladding loss at the pump wavelength, which was caused by the absorption band of Sm-doped ions centered at 940 nm. In the current fiber, the net absorption near 915 nm was about 0.3 dB/m, and the estimated absorption of Sm^{3+} ions at this wavelength was ~0.11 dB/m. This means that Yb absorption at this wavelength was about 0.19 dB/m—only two times higher than the absorption of Sm^{3+} ions. As a result, a significant part of the pump power was lost in the current fiber due to the absorption of Sm^{3+} ions. Similar to the previous factor, increasing the Yb concentration reduced the optimal fiber length and simultaneously reduced the influence of Sm^{3+} ion absorption at the pump wavelength.

It can be seen that both factors noticeably decreased the output power of our amplifier. However, the possible solution in both cases is to increase the Yb concentration in the core. It will shorten the Yb-doped fiber length and significantly reduce the influence of excess loss at signal and pump wavelengths on the PCE. On the other hand, we could not make the Yb concentration very high. In this case, the gain for ASE near 1030 nm became too high, and the optical loss of ~10 dB/m, which was achieved around 1030 nm by bending the fiber, might not be enough to efficiently suppress ASE near 1030 nm. Thus, there could be an optimum of the Yb content in the core glass.

To optimize the fiber parameters, we modeled the amplifier based on the current fiber design for different concentrations of Yb^{3+} ions in the core. For this purpose, we solved rate equations [11], taking into account ASE near 1030 nm. The signal wavelength was taken as 976.5 nm, the pump wavelength was taken as 915 nm, and the core diameter was 13 µm. The cladding diameter was assumed to be 104 µm, which corresponded to the average radius of the fiber with a square-shaped cladding of 92 × 92 µm. The Yb concentration in the glass network was estimated from the measured absorption value at the pump wavelength and was assumed to be 4.5×10^{24} m^{-3}. The model took into account the actual distribution of Yb^{3+} ions across the fiber cross-section (the central part of the fiber was not doped with Yb)—the distribution of inversion along the radius was calculated for each position along the fiber. Absorption and emission cross-sections were borrowed from [12] for aluminosilicate glass.

First, we created a model of the current amplifier. It could be seen that, for the case of the straight fiber, we obtained an optimal fiber length very close to that obtained in the experiment. At the same time, the calculated efficiency for the straight fiber was about 1.5 times higher than that obtained in the experiments. The exact reasons for this discrepancy are not clear. We suggest that it might be due to the non-uniform broadening of the Yb^{3+} absorption band near 976 nm. This effect was previously observed in [5,6], and in [5], it was suggested that it could be a reason for the decrease in efficiency in fiber amplifiers (compared to the free-running fiber lasers). In the current work, our aim was to estimate the influence of Yb concentration on PCE; thus, we compared only the relative change in efficiency, keeping in mind that the real efficiency could be somewhat smaller.

Our calculations showed that the presence of optical loss at the pump wavelength noticeably decreased pump power (compare solid and dash curves for pump). As a consequence, the amplified signal power was reduced by ~30% (compare straight and regular fibers in Figure 6a). Bending of the fiber almost completely suppressed ASE at 1030 nm, but it did not affect the pump-to-signal conversion efficiency too much (see Figure 6b). It is more or less similar to our experiment in which the output power was increased, but only by ~10%.

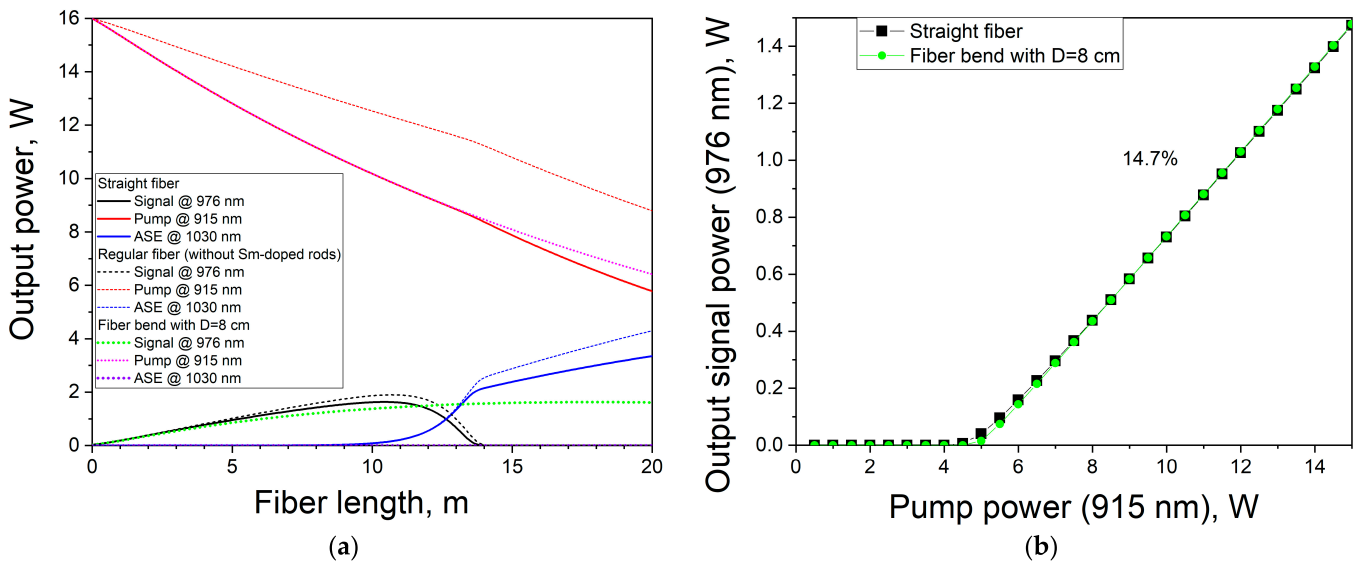

Figure 6. (**a**) Calculated distribution of signal (976 nm), pump (915 nm), and ASE (1030 nm) over fiber length for the case of straight fiber (signal loss @ 976 nm = 0.02 dB/m; pump loss @ 915 = 0.11 dB/m; ASE loss @ 1030 nm = 0.02 dB/m); regular fiber (signal loss @ 976 nm =0.02 dB/m; pump loss @ 915 = 0.02 dB/m; ASE loss @ 1030 nm = 0.02 dB/m); and bend fiber (signal loss @ 976 nm = 0.2 dB/m; pump loss @ 915 = 0.11 dB/m; ASE loss @ 1030 nm = 10 dB/m). (**b**) Dependence of the amplified signal (976 nm) on pump power for the cases of straight fiber and bend fiber.

Then, we calculated the dependence of the slope of the pump-to-signal conversion efficiency (PCE) on the Yb concentration. For each Yb doping level, we modeled fibers with different lengths and found an optimal one that provided maximum output signal. This length was used to define the PCE. The results of our calculations (dependence of PCE on Yb concentration) are shown in Figure 7a. The dependence of the output signal on the pump power for two fiber designs (with core D = 10 μm and 18 μm) with optimal Yb concentration (giving the maximum output power) is shown in Figure 7b. It can be clearly seen that the dependence is very close to linear (similar to fiber lasers), which is a feature of amplifiers operated in the saturation regime. A wide pump power range, in which the amplifier is saturated using a signal power of only 30 mW, was the result of a very high gain at 976 nm. In Figure 7a, we used the relative Yb concentration (Yb concentration in our current fiber was set as 1) for convenience. It could be clearly seen that, for a regular fiber (fiber with optical loss at signal, pump, and ASE wavelengths of 0.02 dB/m), the dependence on Yb concentration was almost constant, except for the region of low concentration, where gray loss became the main factor limiting the efficiency. A similar behavior, but with a decrease in efficiency at a lower Yb concentration, was observed for the straight fiber. It had the same parameters as regular fiber, but an actual pump loss of 0.11 dB/m (due to the absorption of Sm ions) was taken into account. The bent fiber showed great improvement in efficiency (by ~2 times as compared to the regular fiber) at the Yb concentration level, which was three times higher than the current one. Thus, the main approach for efficiency improvement could be to increase the Yb concentration in the core by three times as compared to the current fiber.

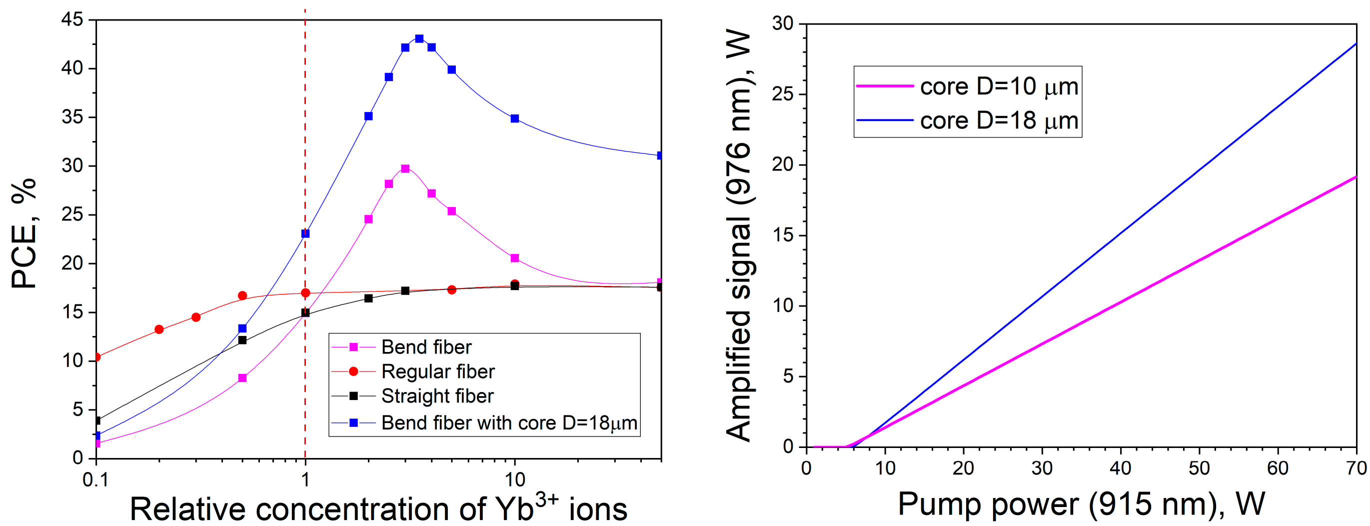

(**a**) (**b**)

Figure 7. (**a**) Calculated dependence of pump-to-signal conversion efficiency (PCE) on the relative concentration of Yb^{3+} ions (one corresponds to the Yb^{3+} ions concentration of $4.5 \cdot 10^{24}$ m^{-3}) for straight fiber (signal loss @ 976 nm = 0.02 dB/m; pump loss @ 915 = 0.11 dB/m; ASE loss @ 1030 nm = 0.02 dB/m); regular fiber (signal loss @ 976 nm = 0.02 dB/m; pump loss @ 915 = 0.02 dB/m; ASE loss @ 1030 nm = 0.02 dB/m); bend fiber (signal loss @ 976 nm = 0.2 dB/m; pump loss @ 915 = 0.11 dB/m; ASE loss @ 1030 nm = 10 dB/m); and bend fiber with a core diameter increased to 18 μm (signal loss @ 976 nm = 0.2 dB/m; pump loss @ 915 = 0.11 dB/m; ASE loss @ 1030 nm = 10 dB/m). (**b**) Calculated output power via pump power for two fiber designs (with core D = 10 μm and D = 18 μm) bent with optimal diameters and with optimal Yb^{3+} concentrations in the core. The parameters of the Yb-doped fibers were signal loss @ 976 nm = 0.2 dB/m; pump loss @ 915 = 0.11 dB/m; and ASE loss @ 1030 nm = 10 dB/m.

Further improvement is possible by increasing the core-to-clad ratio. This is a well-known factor that could improve the PCE in fiber lasers that operate near 976 nm [1–3,7]. With our fiber design, this method could be used even more efficiently due to the tight fiber bending (and the filtering of high order modes) and the additional loss of high-order mode loss due to coupling with high-index rods [13]. Our calculations show that increasing the core diameter to 18 μm will result in an additional increase in PCE of about 1.5 times (see blue curve).

It is quite interesting to note that the proposed technique is also quite promising for another type of amplifiers—Nd-doped fiber amplifiers that operate near 915 nm. In this case, exactly the same problem, i.e., the appearance of unwanted ASE near 1060 nm, typically limits the maximum efficiency. The suppression of ASE near 1060 nm can result in a strong increase in PCE [14,15], but until now, the fiber design that allows it to be implemented has been quite complicated in practice. With the fiber design studied in the current work, we could expect much smaller excess loss due to the much larger distance between the signal wavelength (915 nm) and the ASE wavelength (1064 nm). In addition, Sm^{3+} ions have no absorption at 808 nm, where Nd-doped fibers are typically pumped. This means that both factors limiting PCE in Yb-doped fibers are negligible in the case of Nd-doped amplifiers that operate near 915 nm.

5. Conclusions

In this work, a novel fiber design with controllable position of the stop-band in active fiber configuration (core was doped with Yb) was realized for the first time. The fiber was tested in an amplifier set-up operating near 976 nm. It was shown that unwanted ASE near 1030 nm in this case could be almost completely suppressed by shifting the stop-band to the region of 1000–1100 nm by appropriate bending of the developed fiber. The increase in output laser power was clearly demonstrated compared to a case where ASE was not suppressed. At the same time, two factors that severely limited the maximum achievable pump-to-signal conversion efficiency were revealed: excess loss at the signal wavelength due to the edge of the stop-band and excess loss at the pump wavelength due to absorption of Sm^{3+} ions. The following methods for the significant improvement of PCE efficiency (by more than two times) were discussed: optimization of Yb concentration in the core and optimization of the core–cladding ratio. It was also pointed out that the proposed fiber design is very promising for Nd-doped fiber amplifiers that operate near 915 nm, since both negative factors (excess loss at signal and pump wavelengths) become negligible in this case.

Author Contributions: Conceptualization, M.E.L., S.S.A. and M.M.B.; methodology, M.E.L. and S.S.A.; software, S.S.A. and S.V.A.; validation, D.A.D., V.V.V. and D.S.L.; formal analysis, D.A.D., S.S.A. and M.E.L.; investigation, S.S.A., D.A.D., V.V.V., L.D.I., M.V.Y. and D.S.L.; resources, D.S.L. and M.E.L.; data curation, S.S.A., D.A.D. and M.E.L.; writing—original draft preparation, M.E.L. and S.S.A.; writing—review and editing, A.A.U., L.D.I. and D.S.L.; visualization, D.A.D., S.S.A. and M.E.L.; supervision, M.M.B., D.S.L. and M.E.L.; project administration, M.M.B. and M.E.L.; funding acquisition, M.M.B. All authors have read and agreed to the published version of the manuscript.

Funding: This research was funded by Russian Science Foundation, grant number 21-19-00528.

Institutional Review Board Statement: Not applicable.

Informed Consent Statement: Not applicable.

Data Availability Statement: Data are contained within the article.

Acknowledgments: Authors thank the staff of the large-scale research facilities "Fibers" (UNU Fibers) of GPI RAS for the fabrication and characterization of the used fibers.

Conflicts of Interest: The authors declare no conflict of interest.

References

1. Boullet, J.; Zaouter, Y.; Desmarchelier, R.; Cazaux, M.; Salin, F.; Saby, J.; Bello-Doua, R.; Cormier, E. High power ytterbium-doped rod-type three-level photonic crystal fiber laser. *Opt. Express* **2008**, *16*, 17891–17902. [CrossRef] [PubMed]
2. Röser, F.; Jauregui, C.; Limpert, J.; Tünnermann, A. 94 W 980 nm high brightness Yb-doped fiber laser. *Opt. Express* **2008**, *16*, 17310–17318. [CrossRef] [PubMed]
3. Leich, M.; Jäger, M.; Grimm, S.; Hoh, D.; Jetschke, S.; Becker, M.; Hartung, A.; Bartelt, H. Tapered large-core 976 nm Yb-doped fiber laser with 10 W output power. *Laser Phys. Lett.* **2014**, *11*, 045102. [CrossRef]
4. Li, W.; Matniyaz, T.; Gafsi, S.; Kalichevsky-Dong, M.T.; Hawkins, T.W.; Parsons, J.; Gu, G.; Dong, L. 151W monolithic diffraction-limited Yb-doped photonic bandgap fiber laser at ~978nm. *Opt. Express* **2019**, *27*, 24972–24977. [CrossRef] [PubMed]
5. Matniyaz, T.; Li, W.; Kalichevsky-Dong, M.; Hawkins, T.W.; Parsons, J.; Gu, G.; Dong, L. Highly efficient clad-ding-pumped single-mode three-level Yb all-solid photonic bandgap fiber lasers. *Opt. Lett.* **2019**, *44*, 807–810. [CrossRef] [PubMed]
6. Aleshkina, S.S.; Lipatov, D.S.; Kochergina, T.A.; Velmiskin, V.V.; Temyanko, V.L.; Kotov, L.V.; Bardina, T.L.; Bubnov, M.M.; Guryanov, A.N.; Likhachev, M.E. All-fibre single-mode small-signal amplifier operating near 0.976 µm. *Quantum Electron.* **2019**, *49*, 919. [CrossRef]
7. Kotov, L.; Temyanko, V.; Aleshkina, S.; Bubnov, M.; Lipatov, D.; Likhachev, M. Efficient single-mode 976 nm amplifier based on a 45 micron outer diameter Yb-doped fiber. *Opt. Lett.* **2020**, *45*, 4292–4295. [CrossRef] [PubMed]
8. Tsai, T.-Y.; Song, Y.-C.; Lee, Z.-C.; Lin, S.-T.; Tang, Y.-C. Realization of a compact 10-W 976-nm ytterbium-doped all-fiber laser. *Opt. Lett.* **2023**, *48*, 5667–5670. [CrossRef] [PubMed]
9. Aleshkina, S.; Yashkov, M.; Salganskii, M.; Velmiskin, V.; Guryanov, A.; Bubnov, M.; Likhachev, M. Spectrally Selective Optical Loss in Fibers With High-Index Rods Embedded Into Silica Cladding. *J. Light. Technol.* **2022**, *40*, 4848–4854. [CrossRef]
10. Yablon, A.D.; Yan, M.F.; DiGiovanni, D.J.; Lines, M.E.; Jones, S.L.; Ridgway, D.N.; Sandels, G.A.; White, I.A.; Wisk, P.; Di-Marcello, F.V.; et al. Frozen-In Viscoelasticity for Novel Beam Expanders and High-Power Connectors. *J. Light. Technol.* **2004**, *22*, 16–23. [CrossRef]
11. Desurvire, E. *Erbium-Doped Fiber Amplifiers: Principles and Applications*; John Wiley & Sons, Inc.: Hoboken, NJ, USA, 2002.
12. Melkumov, M.A.; Bufetov, I.A.; Kravtsov, K.S.; Shubin, A.V.; Dianov, E.M. Lasing parameters of ytterbium-doped fibres doped with P_2O_5 and Al_2O_3. *Quantum Electron.* **2004**, *34*, 843–848. [CrossRef]
13. Aleshkina, S.S.; Kochergina, T.A.; Velmiskin, V.V.; Bobkov, K.K.; Bubnov, M.M.; Yashkov, M.V.; Lipatov, D.S.; Salganskii, M.Y.; Guryanov, A.N.; Likhachev, M.E. High-order mode suppression in double-clad optical fibers by adding absorbing inclusions. *Sci. Rep.* **2020**, *10*, 7174. [CrossRef] [PubMed]
14. Yoo, S.; Soh, D.B.S.; Kim, J.; Jung, Y.; Nilsson, J.; Sahu, J.K.; Lee, J.W.; Oh, K. Analysis of W-type waveguide for Nd-doped fiber laser operating near 940 nm. *Opt. Commun.* **2005**, *247*, 153–162. [CrossRef]
15. Pax, P.H.; Khitrov, V.V.; Drachenberg, D.R.; Allen, G.S.; Ward, B.; Dubinskii, M.; Messerly, M.J.; and Dawson, J.W. Scalable waveguide design for three-level operation in Neodymium doped fiber laser. *Opt. Express* **2016**, *24*, 28633–28647. [CrossRef] [PubMed]